The morphological segregation of galaxies in clusters.

III. The distant cluster Cl0939+4713 (Abell 851)[*]

S. Andreon@1@2[**], E. Davoust@2 and T. Heim@2@3

@1 IFCTR-CNR, via Bassini 15, 20133 Milano, Italy
@2 UMR 5572, Observatoire Midi-Pyrénées, 14 Avenue E. Belin, 31400 Toulouse, France, E-mail: davoust at obs-mip.fr
@3 Ecole Nationale Supérieure de Lyon, 46 Allées d'Italie, 69364 Lyon Cedex 07, France, E-mail: Thomas.Heim at ens.ens-lyon.fr

arXiv:astro-ph/9612027v1 3 Dec 1996

Abstract. We have performed an isophotal analysis of galaxies in the distant ($z = 0.4$) cluster Cl0939+4713 (Abell 851), using post-refurbished *Hubble Space Telescope* images. Morphological type estimates for the galaxies are given. A rigorous comparison of the properties of the types shows that early-type galaxies in Cl0939+4713 are, within the present statistical or systematic errors, indistinguishable from their counterparts in Coma in all their studied properties, namely ellipticity profile, slope of the color-magnitude relation from the near-ultraviolet to the near-infrared colors, mean surface brightness and luminosity function in the restframe photographic J band, homogeneity in color (around the color-magnitude relation). Furthermore ellipticals and lenticulars are separately homogeneous in their mean surface brightness, and have similar relative mean surface brightnesses in both clusters.

Spirals are overabundant in Cl0939+4713 with respect to Coma, but twice less than previously estimated, and are more similar to field spirals than to cluster spirals. We suggest that the differences in the photometric properties of the spirals in the two clusters arise from differences in cluster gas density distribution which ultimately bring star formation in the spirals to a stop in Coma, but not in Cl0939+4713.

The morphological types are segregated along a privileged direction that coincides with the position angle of the major axis of the outer X-ray isophotes in the cluster, just like in Coma and Perseus.

Key words: Galaxies: elliptical and lenticular, cD, – spiral – fundamental parameters – luminosity function, mass function – evolution – cluster: individual: Cl0939+4713 (Abell 851)

1. Introduction

Many observational efforts over a long period of time have been devoted to measuring the evolution of the properties of the Hubble types. This has mainly been done by comparing the properties of the types at large distances (z∼ $0.2 - 0.4$) with a nearby reference sample (see as exceptions, e.g. Courteau, de Jong & Broeils 1996, Zepf 1996).

When comparing the properties of the Hubble types, a first problem came from the difficulty, and in part the subjectivity, in estimating Hubble types. Expert morphologists are able to classify galaxies in morphological types with a reproducibility in the range 50 to 80 % (Andreon & Davoust 1996) when galaxies are classified in three types. The reproducibility is obviously lower when each morphologist uses his personal definitions for the types. Unfortunately, many recent studies of distant galaxies (e.g. Casertano et al. 1995, Glazebrook et al. 1995, Driver, Windhorst & Griffits 1995), but not all (Dressler et al. 1994a,b, Abraham et al. 1996, van den Bergh et al. 1996) use definitions for the types which are not identical to those used by morphologists for nearby galaxies. Morphologists classify (nearby) galaxies by their resemblance to standards (Hubble 1936, de Vaucouleurs 1959, Sandage 1961), whereas distant galaxies are often classified without any reference to standards and in classes that are not easy to link to the traditional ones (for example Glazebrook et al. 1995 classify usual edge-on lenticulars as spirals, and put together in one class compact galaxies and ellipticals).

Second, the comparison of types at different redshifts has been hampered for a long time by the lack of angular resolution of groundbased telescopes that do not allow imaging distant galaxies with the same restframe spatial resolution as nearby ones, and therefore do not allow one to classify distant galaxies, in spite of great efforts to observe distant galaxies in sub-arcsecond seeing conditions (e.g. Thompson 1986, Lavery, Pierce & McClure 1992). The *Hubble Space Telescope* (*HST*) has now opened a new era and the situation has been partly reversed, since images of distant galaxies are now available with better restframe resolution than for nearby galaxies (see Sect. 3.1 for details).

The goal of this paper is to study the galaxies in Cl0939+4713, a distant cluster observed by the *HST*, to compare their prop-

erties to the ones of galaxies in the Coma and Perseus clusters, presented in previous papers of this series (Andreon 1994, 1996a), in order to gain insight into the epoch dependence of the properties of the Hubble types. This is done using the same method for classifying all the galaxies from images of similar restframe resolution and for samples selected in the same restframe passband down to the same absolute magnitude.

The paper is organized as follows. Section 2 outlines our present understanding of the properties of the galaxy populations in Cl0939+4713. Section 3 deals with the problems that could bias the comparison of morphological types of galaxies at different redshifts. The morphological types of galaxies in Cl0939+4713 are presented and discussed in Section 4. In Section 5 we study the properties of the types, among themselves and with respect to local counterparts, and we devote Section 6 to a discussion and a summary of the results. We adopt $H_0 = 50$ km s^{-1} and $q_0 = 0.5$, but, when appropriate, we discuss the consequences of the adopted cosmological model.

2. The distant cluster Cl0939+4713

Cl0939+4713 (Abell 851) is a distant cluster (at $z = 0.407$) for which a large effort has been made to collect large samples of data at different wavelengths. Dressler & Gunn (1992) give g, r, i magnitudes, $g - r, r - i$ colors and positions. They also give the redshift of some galaxies. Dressler et al. (1994a, hereafter DOBG) give the morphological types of galaxies in the cluster core, as estimated from pre-refurbished HST images, and a first analysis of the properties of the Hubble types, revealing the ordinariness of these galaxies from the point of view of their morphology, from their location in the color-magnitude diagram, from the usual luminosity function and from the spatial distribution of the morphological types.

Dressler et al. (1994b) present post-refurbished HST images of this cluster and re-classify the galaxies, but they do not give their morphological estimates. The comparison of the HST morphological type estimates, before and after refurbishing, performed by Dressler et al. (1994b), shows that the two estimates differ for only 20 % of the sample.

In a narrow-band study, Belloni et al. (1995) and Belloni & Röser (1996) point out the presence of numerous E+A galaxies, and that their radial distribution is less concentrated than those of early-type galaxies.

Stanford, Eisenhardt & Dickinson (1995) give the infrared colors of galaxies in an area that is much larger than the HST field of view, but limited to a bright magnitude ($K = 18$ mag). They find that the redder galaxies are bluer than present day Es and S0s by a quantity which is compatible with the blueing expected for passive galaxy evolution. Furthermore, the subsample of early-type galaxies with known morphological types has a small scatter around the color-magnitude relation in the visual and near-infrared colors; this is indicative of the homogeneity of its photometric properties at these wavelengths. However, the early-type galaxies seem not to have the expected $J - K$ and $H - K$ colors, as they have brighter H and lower J fluxes for their K magnitude.

In the effective radius vs effective surface brightness plane, the 14 galaxies of this cluster with known surface brightness parameters occupy the same locus as local early-type galaxies (Pahre, Djorgovski & de Carvalho 1996). Barrientos, Shade &

Lópèz-Cruz (1996) instead suggest that, for a given size, early-type galaxies in Cl0939+4713 are brighter than the Coma ones, and note that this small discrepancy with the results of Pahre, Djorgovski & de Carvalho (1996) is within the systematic errors of the two works.

In the X-rays, the cluster looks irregular, as it is azimuthally asymmetric (Schindler & Wambsganss 1996). Seitz et al. (1996) present the two-dimensional mass distribution constructed from weak lensing on background galaxies and find that mass follows light.

3. Problems in the comparison of types at different redshifts

Comparing the properties of a given Hubble type in different environments is a non trivial task when very different observational materials are used for classifying the galaxies, and the images taken with the Wide Field Camera 2 of the HST differ in many respects from images taken with groundbased telescopes. The selection criteria and the classification methods may also differ. In the next sub-sections we detail the problems that arise because of these differences, and explain how we solved them.

3.1. The comparison sample

The Hubble type estimates depend on the resolution of the images used for classifying the galaxies (de Vaucouleurs & Buta 1980, Poulain, Nieto & Davoust 1992). The resolution of the HST images for the Wide Field Camera 2 is 0.1 arcsec (FWHM) which corresponds to 0.65 Kpc in the restframe of galaxies at $z \sim 0.4$. For a meaningful comparison, such a resolution in Kpc is needed for the nearby comparison samples as well.

This perfect sample does not exist, so we settled for the next best thing, two samples of galaxies in Coma (Andreon et al. 1996a,b). The two samples are composed of 187 galaxies brighter than $M_J = -19.8$ mag within one degree from the cluster center (hereafter the Coma-whole sample) and a deeper sample of 96 galaxies brighter than $M_J = -19.3$ mag within a central circular region of 15 arcmin in radius offcentered from the cluster center by 21 arcmin (hereafter the Coma-center sample). These two samples exceed in size that of Saglia, Bender & Dressler (1993).

The angular resolution of the galaxy images is not uniform; it is broadly distributed, and centered at 0.78 Kpc. By comparing Hubble type estimates determined from images with different resolutions, some better than 0.65 Kpc, we have shown that the Hubble type estimate is not sensitive to small differences in resolution around 0.65 Kpc (Andreon et al. 1996b, Andreon & Davoust 1996). The resolution of our comparison sample can thus be considered sufficient for our purpose.

3.2. Sampling and shape of the point spread function

Sampling and contrast are two basic ingredients for recognizing morphological components of galaxies, such as bar, disk, spiral structure and, more generally, deviations of the isophotes from the perfect elliptical shape.

Even in the ideal case when the resolution in Kpc is the same for the nearby and the distant galaxies, the image qualities still differ, because the sampling and the shape of the point spread functions are not equal. The FWHM of the *HST* point spread function is sampled with only one pixel, whereas the FWHM of the groundbased point spread function is sampled with typically 3 to 4 pixels. This fact induces some differences in the Hubble type estimates for galaxies of the same Hubble type observed from the ground or from space.

We have performed simple (i.e. noiseless) two-dimensional simulations of the appearance of structural components such as halo, bar, bulge, disk, etc. when observed with the Wide Field Camera 2 and from the ground (Andreon 1996b). They show that we do not lose *large* structural components, such as the disk, the envelope or the spiral pattern of distant galaxies (brighter than $M_J = -19.0$ mag) observed with the Wide Field Camera 2 more than we do for nearby galaxies observed from the ground. Therefore, galaxies of the same Hubble type will be put in the same coarse class (i.e. E, S0, S).

But they also show that *small* details, such as a bar, or small deviations from the perfect elliptical shape, those allowing the classification of ellipticals as boxy or disky and of lenticulars as barred or unbarred, are more likely to be lost with *HST* images of distant galaxies than with groundbased images of nearby galaxies. Therefore, the relative proportions of ellipticals or lenticulars of the two subtypes measured in distant clusters are not comparable with those in nearby clusters.

To be more specific, if the Coma barred lenticulars were artificially placed at the distance of Cl0939+4713, the major axis of their bar would be 0.3 to 0.4 arcsec (i.e. 3 to 4 pixels) long on average. It is very difficult to measure the change in position angle of such a short major axis and the simultaneous increase of ellipticity, which are distinctive features of a bar. Such result cannot be extrapolated to bars in spirals, which are morphologically different, and therefore to the bulk of the galaxies of the Hubble Deep Field. Incidentally, we note that only a very small fraction of barred galaxies has been detected in Cl0939+4713 by us (see column 10 of Table 1).

The arms of flocculent spirals are more likely to be lost in Wide Field Camera 2 images, as already noted by Ellis (1996), thus introducing another possible bias between groundbased and space observations. But we have two reasons to think that the fraction of misclassified flocculent spirals is small: first of all, these galaxies often have HII regions, in which case they are correctly classified as spirals; second, flocculent spirals are not frequent in the center of clusters, even less so than grand design spirals (at least in clusters at zero redshift).

3.3. Pass-band: selection and absolute magnitude limit

The Hubble type composition depends on the pass-band in which the sample has been selected, since samples selected in the blue are richer in spirals than those selected in the red.

The galaxies in Cl0939+4713 were observed and selected through the $F702W$ filter, large (1950 Å) and centered at $\sim$ 6900 Å, (Holtzmann et al. 1995) which samples the restframe emission at $\lambda \sim 4900$ Å with a bandwidth of 1390 Å.

Galaxies in nearby clusters are often selected in the photographic J filter (and in particular our major comparison sample, the Coma cluster, was selected in a J-like band), which is centered at 4600 Å with a bandwidth of 1500 Å, approximately matching the emission sampled by the $F702W$ filter

for distant galaxies. Therefore we can use different filters for selecting samples in approximately the same restframe passband, as has been done, for example, by Aragón-Salamanca et al. (1993) and Rakos & Schombert (1995) for other filters.

The $F702W$ magnitudes for the galaxies in Cl0939+4713 were taken from Seitz et al.'s (1996) catalogue (kindly made available by J.-P. Kneib). Two bright galaxies are clearly missing from Seitz et al.'s catalogue (DG 371, and DG 438; the names are from Dressler & Gunn 1992). These two galaxies have been added to the catalogue and their $F702W$ magnitudes have been estimated from the Gunn r magnitudes assuming for their $r - F702W$ color the median value (0.505 mag) of all the galaxies in common between Seitz et al. (1996) and Dressler & Gunn (1992).

The b_{GMP} magnitudes (which are magnitudes measured through a J−like filter but with the Johnson B photometric zero point) of the Coma galaxies listed by Godwin, Metcalfe & Peach (1983) are re-transformed to J by the relation

$$J = b_{GMP} - 0.57$$

computed from the comparison of the b_{GMP} and J magnitudes, the latter taken from Butcher & Oemler (1984) for 148 galaxies in common with our sample of 187 with $b_{GMP} < 16.5$. This transformation takes into account the difference in the zero point between the two systems, and it is not a color transformation, since both magnitudes map the same wavelength range.

We now determine the zero-point shift between the $F702W_{z=0.4}$ and $J_{z=0}$ systems, in order to select the distant and nearby samples down to the same limiting absolute magnitude.

We compute the $F702W - J$ color at redshift zero and the K corrections in $F702W$ by convolving the galaxy spectral energy distributions listed in Coleman, Wu & Weedman (1980) with the $F702W$ (at http://www.stsci.edu/ftp/instrument) and J_k (J.-M. Miralles, private communication) filter shapes, and by normalizing the $F702W - J$ color at redshift zero of ellipticals to the one listed in Fukugita, Shimasaku & Ichikawa (1995). We find:

$$F702W_{z=0.4} - J_{z=0} = -0.95 \quad \sigma = 0.1$$

where σ indicates the scatter between the four different spectrophotometric types (E/S0, Sbc, Scd, Irr). Since there is a small residual dependence between the spectrophotometric type and the photometric transformation due to the slightly redder sampling of the $F702W_{z=0.4}$ filter with respect to the $J_{z=0}$ filter, we still include less Irr and more E/S0 when selecting the galaxies in the $F702W_{z=0.4}$ band than we would when observing the Cl0939+4713 galaxies exactly in the J restframe. We quantify this (negligible) effect in Sect. 4.

3.4. Pass-band: classification

The morphological classifications in Coma and Cl0939+4713 are not performed in the same restframe passband, and therefore there could be systematic differences in the morphological classification because of the passband dependence of the contrast of spiral arms and dust with respect to the galaxy main body.

However, such systematic differences apply only to a minority of galaxies, those whose type is on the borderline between two classes, and we verified that the passband dependence of the morphological type, at the sampled wavelengths, is negligible for galaxies at low redshift.

3.5. Definition of the used Hubble types

It is clear that, whatever definition of the Hubble types is adopted, it must be the same for distant and for nearby galaxies, which implies that the method used for classifying the galaxies has to be the same in both cases, although this requirement is not always satisfied in the literature (see the Introduction).

The method introduced by Michard & Marchal (1993), which allows one to assign Hubble types to galaxies according to the presence or absence of morphological components, such as bar, disk, bulge, halo, dust or spiral arms, gives reproducible morphological estimates and has the advantage that it has already been applied to galaxies of the local Universe (Michard & Marchal 1994 and reference therein, Andreon 1996b), and in particular to our two Coma samples (Andreon et al. 1996a,b). Therefore we decided to use this method to classify the galaxies of Cl0939+4713 as well.

In this scheme, ellipticals are galaxies with elliptical isophotes and almost linear surface brightness profiles in the μ vs. $r^{1/4}$ plane, lenticulars have elliptical isophotes, but their major axis surface brightness profile presents a bump, and, finally, spirals do not have elliptical isophotes. Galaxies not following these typical trends are not classified. Details can be found in Michard & Marchal (1993) and Andreon & Davoust (1996).

3.6. Membership

It is important to remove background or foreground galaxies from the sample when we are interested in the properties of the galaxy population in a selected region of the Universe.

At small distances, galaxy redshifts are available for most samples, and one can therefore reject interlopers on the basis of their velocity relative to the cluster center. We did this for the two samples in Coma (Andreon 1996a and Andreon et al. 1996a).

In Cl0939+4713, redshifts are available for only a small number of galaxies (25 out of 83 brighter than $F702W = 22.2$ mag in the field of view), and the membership of galaxies must be determined in a different way.

In this field, we statistically expect eleven background or foreground galaxies brighter than $F702W = 22.2$ mag from the counts-magnitude relation of Smail et al. (1995), whose integral is normalized at $F702W = 27$ mag as in Seitz et al. (1996). We have identified nine of them with certainty (DG 234, DG 349, DG 396, DG 398, DG 403, DG 407, DG 420, DG 440 from their redshifts and DG 380 because it is interacting with DG 398, an interloper). Three other galaxies (DG 292, DG 384 and DG 385) are suspected of being background quasars (see Sect. 4). We have therefore identified 12 probable (most of them certain) background or foreground galaxies; since 11 were expected, it is reasonable to assume that all the other galaxies in the field of view (brighter than $F702W = 22.2$) are cluster members. We have identified almost all non member galaxies, in spite of the small fraction of galaxies with known spectrum (1/3), because DG chose to take spectra of blue galaxies.

We can confirm in an independent statistical way that the sample is not significantly contaminated by interlopers, using spectrophotometric redshifts taken from Belloni & Röser (1996), as if they were redshifts based on emission or absorption lines. The spectrophotometric redshifts exclude seven galaxies from our sample, but do not exclude seven others which are interlopers by their kinematic redshift.

Therefore, the resulting sample is likely to be an absolute magnitude complete sample of galaxies, like the two Coma ones.

4. The morphological types of galaxies in Cl0939+4713

In order to exclude from the sample galaxies partially outside the field of view, the studied field for Cl0939+4713 is ~ 2 arcsec smaller on both sides of the field of view of each of the three CCDs that compose the Wide Field Camera 2.

With the images of Cl0939+4713 at our disposal, we classify galaxies down to $F702W = 22.2$ mag, corresponding to $M_J = -19.0$ mag, which we conservatively take as our magnitude limit for morphological classification.

Such faint galaxies have not yet been morphologically classified in the Coma cluster, the deeper samples reaching $M_J = -19.3$ mag. Therefore, in the following, when we make comparisons among these samples, we limit the deeper one (Cl0939+4713) to the magnitude of the shallower one.

Table 1[1] presents a concise description of all galaxies brighter than $F702W = 22.2$ mag in the HST studied field of view with the exclusion of certain background/foreground galaxies. We present the morphological type (column 14), a characterization of the galaxy envelope (column 13) and many other geometrical parameters, detailed in the legend of Table 1, together with notes to the individual galaxies.

We did not succeed in attributing a morphological type to only 8 galaxies out of 71.

Three of them are morphologically unresolved galaxies, i.e. resolved sources but not large enough to be assigned a morphological type. These galaxies have small radii for their magnitude. They are, from the morphological point of view, very similar to the quasar DG 440 at $z \sim 2$, present in our field, which suggests that they could be background quasars. For this reason we exclude them from the sample. This decision does not affect our comparison of Hubble types since these galaxies are certainly not ellipticals, lenticulars or spirals. This decision affects only marginally our comparison of the whole population of galaxies in Cl0939+4713 with the Coma cluster one, because, if these galaxies do belong to Cl0939+4713, one is fainter than the absolute magnitude limit of the Coma-center sample, and three are fainter than that of the Coma-whole samples. They are therefore already excluded from the comparison sample because they are too faint.

Five other galaxies are classified as peculiar. Three of them (DG 311, DG 318 and DG 436) present features typical of interacting galaxies, such as tidal arms. Among these three galaxies, the brightest cluster galaxy (DG 311) shows a tidal arm of very low contrast (and unusual $g - r$ and $r - i$ colors), but a normal surface brightness profile and elliptical shape (at small radii). The two other galaxies (DG 137 and DG 339) present pear-shaped isophotes and a detailed morphology that we did not find in any Coma galaxy, but again one is fainter than the absolute magnitude limit of the Coma-center sample, and both are fainter than that of the Coma-whole sample.

---

[1] Table 1 is presented only in electronic form

4.1. Similarity with present day galaxies

The fact that a Hubble type can be assigned to almost all galaxies of Cl0939+4713, even with classification criteria as strict as ours, reinforces DOBG's impression of the ordinariness of galaxies of Cl0939+4713. First of all, the galaxies with elliptical isophotes have de Vaucouleurs-like surface brightness profiles, as present day ellipticals, or a bump along the major axis, as lenticulars. When this bump is present, it is always linked to a change in the isophote axis ratio, as for present day lenticulars. The $e_4{}^2$ profile of distant lenticulars is similar to that of present day ones. In other words, distant and nearby galaxies with similar surface brightness profiles also have similar ellipticity and e_4 profiles. The similarity between lenticulars holds even on a statistical basis: the proportion of lenticulars of Cl0939+4713 with a decreasing, stationary or increasing outer ellipticity profile (which leads to the envelope classification of exD, thD, spH in Table 1; see Michard & Marchal 1993 and Andreon 1996b), is the same as in Coma (0%/50%/50%).

Furthermore, in early-type galaxies, the more important (i.e. larger) coefficient measuring the deviation of the isophotes from the perfect elliptical shape is the e_4 parameter, as for present day early-type galaxies.

The similarity of distant galaxies to local counterparts holds for the shape of the broad spectrum too. Distant and nearby early-type galaxies have the same spectrum. Distant spirals present a variety of spectra, as present day spirals. In fact, comparing our morphological types to the spectrophotometric types of Belloni & Röser (1996), we found that, out of 36 early-type galaxies, 34 have the spectrum of an early-type galaxy, one that of an Sbc and the last one that of an E+A. Out of 29 spirals, 11 have the spectrum of an S/Im, 10 an early-type spectrum and 8 are E+A's. A similar conclusion has been reached by Belloni et al. (1995) in their comparison of their spectrophotometric type to DOBG's morphological types. Similarly, the break at 4000 Å (taken from the same reference) is more prominent in Es than in Ss, as in the local universe (Belloni & Röser 1996).

4.2. Comparison with pre- and post-refurbished types

The comparison between DGOB's morphological type estimates and ours, from pre- and post-refurbished *HST* images respectively, shows that the two types are compatible, once differences in the observational material are taken into account, for example our detection of a disk or a spiral pattern that DGOB do not see because of the lower quality of their data. Galaxy to galaxy comparisons are presented in the "Notes to the galaxies" in Table 1 for remarkable cases.

Post-refurbished *HST* morphological types for 31 galaxies, estimated by Dressler et al. (1994b) are listed in Stanford, Eisenhardt & Dickinson (1995). We attribute the same morphological label to 24 (77%) of them. The morphological type of the other galaxies differs by one class (i.e. no Es in one study have been classified as Ss in the other one), and we have a tendency to classify the galaxies into a slightly later type than Dressler et al. (1994b). The latter authors present a similar

---

rate of agreement among themselves. The rate of agreement between our types and Dressler et al.'s (1994b) for Cl0939+4713 is the same as that between our types and those from other authors for Coma galaxies (Andreon & Davoust 1996), including Dressler.

Please note that, since our method for estimating the Hubble type is the same for both nearby and distant galaxies and it is highly reproducible, this comparison does not measure the reproducibility of our Hubble type estimates but only how similar our classification system is to the other one.

4.3. Morphological composition of Cl0939+4713

Table 2. Morphological composition of Coma and Cl0939+4713 for various cluster regions and magnitude limits

Region	N_{gal}	Percentage of			
		E	S0	S	other
$M_J = -19.0$					
Cl0939+4713	71	14	37	42	7
$M_J = -19.3$					
Cl0939+4713	67	15	34	43	7
Coma-center	96	23	52	19	6
$M_J = -19.8$					
Cl0939+4713	52	13	31	48	7
Coma-center	71	27	48	21	4
Coma-whole	186	25	42	31	2
(Coma-center)^C ∩ (Coma-whole)	115	24	39	37	-

Note: (Coma-center)^C is the complementary of the Coma-center sample.

Table 2 presents the morphological composition of Cl0939+4713 in the studied region down to our limiting magnitude for morphological classification ($M_J = -19.0$ mag) and down to the adopted limits for galaxy classification of two comparison samples. Note that the area surveyed by the field of view of the *HST* has a radius which is half that of the Coma-center sample.

Down to both common absolute magnitudes, the spiral fraction of Cl0939+4713 is $\sim 20\%$ higher than in Coma, and lenticulars are less abundant by 10 to 20 %. Ellipticals are $\sim 10\%$ less abundant in Cl0939+4713 than in Coma.

The fact that the $F702W$ filter does not exactly match the redshifted J galaxy emission has a negligible influence, since our numbers of galaxies change by 1 on the average when differentially shifting by 0.1 mag the luminosity function of one or two morphological types.

DOBG compare the morphological composition of Cl0939+4713 to the "typical" one of rich clusters and of the field. They find a larger difference than we do between the spiral composition of Cl0939+4713 and that of nearby clusters. But their estimate of the spiral fraction in nearby clusters is smaller than what we find in Coma; this is expected because of the general tendency of morphologists to underestimate the spiral fraction of nearby clusters, which we have shown to exist in Coma, Perseus and other nearby clusters (Andreon 1993, 1994, 1996a, Andreon & Davoust 1996). The main reason for the disagreement between

---

[2] The e_4 parameter (often called a_4 in the literature), when positive, points out an excess of brightness along the major axis of the galaxy, with respect to a galaxy with perfect elliptical isophotes.

DOGB and us is that the images used by morphologists to classify galaxies in nearby rich clusters generally have a lower resolution than that necessary for a well controlled comparison, as explained in Sect. 3.1. Also, DOBG compare the morphological fraction of Cl0939+4713 down to $M_J \sim -18.1$ mag to that of nearby clusters down to an unspecified absolute magnitude. Since no morphological types have been published for such faint galaxies in rich nearby clusters, their comparison sample must be limited to a brighter absolute magnitude, thus invalid, unless they used unpublished observations of a deep sample.

From the inspection of Figure 5 of DOBG, we note that many faint galaxies in Cl0939+4713 are spirals. Therefore, using a brighter limiting magnitude for the Cl0939+4713 galaxies, similar to ours and to that used for rich nearby clusters, DOBG would probably find a lower proportion of spirals in Cl0939+4713, comparable to ours, and closer to the one estimated for nearby clusters. At any rate, they agree with us on the spiral fraction for the 31 galaxies in common.

Therefore, the morphological composition of Cl0939+4713 does indeed differ from the one of nearby clusters, but *by a factor two less* than what is found by DOBG. The necessity of a morphological evolution of galaxies in clusters is thus strongly reduced. This is discussed in Sect. 7.3.

5. The properties of the Hubble types

Galaxies which are morphologically similar are not necessarily similar in their physical properties, especially when they have different ages (i.e. when they are at different redshifts). In other words, the similarity of morphological composition of Cl0939+4713 and Coma does not imply that the galaxies in the two clusters have the same physical properties. To verify this possibility, we must compare the luminosity function, color and surface brightness distributions, morphological segregation, and other properties of the morphological types of the two samples.

5.1. Astrophysical parameters and method of analysis

The following physical parameters of the Cl0939+4713 galaxies were considered.
– Positions, $F702W$ isophotal magnitude, isophotal area at the 25.3 $F702W$ magnitude arcsec^{-2} were taken from Seitz et al. (1996) for all but three galaxies. The $g - r$ and $r - i$ colors were taken from DG92 for all but two galaxies. This sample is selected in the $F702W$ filter ($\sim J$ restframe) and is practically 100 % complete (for galaxies of normal central brightness, i.e. $J < 25$ mag arcsec^{-2}).
– The infrared magnitudes J, H, K and through an intermediate filter centered at 7840 Å, referred to as visual, came from Stanford, Eisenhardt & Dickinson (1995) for 46 galaxies selected for having $K < 18.00$ mag and in the HST field of view. This sample, selected in K, is expected to be ~ 90 % complete in magnitude down to $K = 18$ mag.
– The morphological types of the galaxies came from Table 1.

The panels of Fig. 1 show the spatial distribution of all the galaxies and for the three morphological types. Spirals are uniformly distributed, lenticulars are mainly found in the two upper CCDs and Es in the upper halves of these two upper CCDs.

We then computed the following quantities and their distribution for each morphological type.

– the positions (x, y); they are Seitz et al.'s positions rotated clockwise by 20 degrees around the cluster center adopted by us (the dominant galaxy DG 311), to align the x and y axes with the privileged directions suggested by the spatial distribution of the galaxy types (see Fig. 1);
– The the clustercentric distance and the angle with respect the privileged direction (θ);
– the luminosities and $(g - r, r - i, J - H, H - K, visual - K)$ colors; for the infrared colors we split the sample in only two classes, (E+S0) and S, because of low statistics;
– the local density, defined as the density inside the smallest circle containing the 10 nearest galaxies (Dressler 1980), the distance to the nearest neighboring galaxy (d_1); they were computed using Dressler & Gunn's (1992) catalogue, limited to the Gunn $r = 22.7$ mag in order to avoid border effects in the density and the distance to the nearest neighboring galaxy computations;
– the mean surface brightness, $<$SuBr$>$; it was computed taking into account the galaxy ellipticity. This parameter is missing for the two galaxies not present in the Seitz et al. catalogue (DG 371 and DG 438, see Sect. 3.3).

The method used to test the reality of the differences (if any) between the galaxy properties along the Hubble sequence has been presented and thoroughly tested in Andreon (1994, 1996a,b). In summary, the probability that an observed difference between the distributions of a given quantity for two types is real (or, better, one minus the confidence level for rejecting the hypothesis that the two classes are drawn from the same parental distribution) is computed by 100000 Monte Carlo simulations in which the galaxy types are shuffled randomly. As the number of objects in each class is small, it is important to use robust statistics. We used robust estimates of the distribution moments, even if, for the sake of clarity, we referred to them by their un-robust names (for example the central location index is called mean).

5.2. J Luminosity function

The global luminosity function of Cl0939+4713 has a maximum at $M_J = -20$ mag (Figure 2a, left panel), which is not due to incompleteness of the catalogue, since the limiting magnitude is at least four magnitudes fainter. Our statistical tests show that the global luminosity function of Cl0939+4713 pretty well matches that of the whole cluster down to $M_J = -19.8$ mag and that of Coma's core down to $M_J = -19.3$ mag, our limiting magnitudes (Figure 2a, top-center and top-right panels, and note the absence of any row containing L in Table 3, see the legend of Table 3). The 68 % confidence limits for the differential distance moduli between Coma and Cl0939+4713, inferred from matching the respective luminosity functions are +6.0 and +6.6 mag; they do not exclude any reasonable luminosity evolution, such as the one expected by passive evolution, or value of q_0, since the expected differential distance modulus, for $q_0 = 0.5$, is +6.4 mag.

We do not detect any statistically significant difference between the luminosity functions of the different morphological types of Cl0939+4713 (and there is no line for such a quantity in Table 3); this is in agreement with what we found for a sample of galaxies of approximately the same size in Perseus

Table 3. Probability, expressed in percentage, that two galaxy classes c1 and c2 have the same parental distribution in distance y, azimuthal distance θ, color $g - r, r - i$, mean surface brightness $<$SuBr$>$. Probabilities of other parameters were also tested, but gave null results. Only pairs of morphological types having less than 0.2 % probability to be drawn from the same parental distribution are listed. For the sake of clarity, probabilities larger than 15 % are replaced with blanks. Null results are not listed but are discussed in the text when interesting. The probabilities T, F, TI and SI refer to differences in the mean, dispersion, kurtosis and skewness (the names are those of the classical tests). The probabilities KS and P5 refer to the classical Kolmogorov-Smirnov test and to the vector (T, F, TI, SI, KS) (see Andreon 1994 and 1996a,b for details).

c1	c2	quantity	P5	T	F	TI	SI	KS
E	S0	y	0.175	5.050		2.548		4.952
E	S	y	0.009		5.253	0.209		3.854
E	S	θ	0.147			11.393		
E	S	$g - r$	0.000	0.010	0.001			0.000
S0	S	$g - r$	0.000	0.000	0.000			0.000
E	S	$r - i$	0.001	3.108	0.150			0.020
S0	S	$r - i$	0.000	0.749	2.191		6.667	0.029
E	S0	$<$SuBr$>$	0.109	0.125				0.889
S0	S	$<$SuBr$>$	0.007	0.228				0.768

(brighter than $M_V = -19.5$ mag, Andreon 1994), but at variance with what we found for a larger sample of galaxies in Coma (brighter than $M_J = -19.8$ mag).

The statistical significance of the difference between the luminosity functions of the Cl0939+4713 and Coma types (Es+S0s and Ss) is smaller than 2σ (see also Figure 2a, center and right panels, and note the absence of any row containing L in Table 3), confirming DOBG's suggestion.

There is no statistical evidence, larger than 2σ, for a difference between the luminosity functions of the Cl0939+4713 and Coma types (Es+S0s and Ss) (see also Figure 2a, center and right panels, and note the absence of any row containing L in Table 3), confirming DOBG's suggestion.

5.3. Mean surface brightness

The mean surface brightness distribution of S0s differs from those of Es and Ss, in part because S0s are brighter in the mean (by 0.2 mag arcsec^{-2}) (Figure 2b and Table 3, T column, last two rows).

The measured dispersions in mean surface brightness are 0.23 and 0.18 mag arcsec^{-2} for Es and S0s respectively, and are likely to be due to photometric errors. That is, Es and S0s are separately homogeneous in mean surface brightness within the present photometric accuracy. In fact, an error a 0.1 mag arcsec^{-2} in the determination of the galaxy isophotal brightness, which is possible in our measures, translates into a 0.16 mag arcsec^{-2} error in the mean surface brightness for elliptical galaxies whose effective radius and surface brightness obey the Kormendy (1977) relation.

In Coma, we also found that S0s have a higher surface brightness than Es by 0.2 mag arcsec^{-2}. We cannot compare directly the mean surface brightnesses of the types in Cl0939+4713 and in Coma, since they are computed within different restframe isophotes. We can only say that each of the two classes is homogeneous in the two clusters and that the difference in mean surface brightness between Es and S0s is the same in both clusters. The zero point for the comparison of surface brightnesses at different redshifts is given by Pahre,

Djorgovski & de Carvalho (1996), who found that the early-type galaxies studied in Cl0939+4713 occupy the same locus as the Coma galaxies in the effective radius vs effective surface brightness plane. This implies that Es and S0s in Cl0939+4713 have the same mean surface brightness as the respective classes in Coma.

In the study of the whole Coma cluster, we found that S0s have fainter mean surface brightnesses than Ss, contrary to our finding for Cl0939+4713. However, we are sampling different portions of the two clusters, and the presence of spirals with high surface brightness in Coma is limited to large radii (since overbright spirals are blue and blue spirals avoid the cluster center; see Andreon 1996a), not sampled in Cl0939+4713. Sampling only the core of the Coma cluster (say within a radius of 500 Kpc), as we do for Cl0939+4713, spirals have fainter surface brightnesses than S0s, as in Cl0939+4713.

The dispersion in mean surface brightness of Ss in Cl0939+4713 is larger than for early-type galaxies (0.34 mag arcsec^{-2} vs. $\sim$0.2 mag arcsec^{-2}), as in Coma.

5.4. Optical colors

5.4.1. Early-type galaxies

Es and S0s have the same colors (formally 1.56 and 1.52 mag in $g - r$ and 0.68 and 0.64 mag in $r - i$; see also Figure 2b, and note the absence of any row involving these colors and morphological types in Table 3). In $r - i$, the dispersion is 0.05 and 0.09 mag for ellipticals and lenticulars respectively, and reasonably of the order of the photometric accuracy[3]. In $g - r$, the dispersion around the color-magnitude relation is 0.07 and 0.08 mag for ellipticals and lenticulars respectively, again within the

---

[3]   Dressler & Gunn (1992) do not estimate this quantity. A rough estimate is given by $\sqrt{2}$ times the photometric error in r, which in turn can be estimated from the scatter in $F702W - r$ for early-type galaxies assuming a negligible intrinsic scatter in the $F702W - r$ color and a negligible photometric error in $F702W$, two reasonable assumptions. This give $\sigma \sim 0.08$ mag

photometric accuracy. Therefore, both Es and S0s are homogeneous in these two colors, which sample the $\sim U - B$ and $\sim B - V$ restframe colors. This extends the homogeneity of early-type galaxies from visual and near infrared colors (Stanford, Eisenhardt & Dickinson 1995) to near ultraviolet and blue–visual colors.

The slope of the color-magnitude relation in both $g - r$ and $r - i$ colors (– 0.118 in $g - r$ vs. $F702W$) is compatible with the one of the Virgo cluster (Visvanathan & Sandage 1977), and of other nearby clusters (Garilli et al. 1996), extending to much bluer colors a similar finding by Stanford, Eisenhardt & Dickinson (1995).

Nothing can be said about the normalization of the color-magnitude relation (i.e. about the galaxy colors reduced to a fixed absolute magnitude) because the zero point determination of the colors in Dressler & Gunn (1992) has a large error (0.1–0.2 mag).

The $g - r$ filter samples the 4000 Å break in the galaxy restframe and is therefore sensitive to the galaxy star formation and evolutionary history, whereas the visual and near-infrared colors are more sensitive to metallicity. The homogeneity of the colors of early-type galaxies in Cl0939+4713 strongly suggests a common star formation and evolutive history, as found in the optical colors for Coma early-type galaxies by Bower, Lucey & Ellis (1992). The measured dispersion in the blue color (0.08 mag) for early-type galaxies in Cl0939+4713 is fully compatible with the photometric errors. Using the prescriptions of Bower, Lucey & Ellis (1992), we can put a lower limit on the age of early-type galaxies, which depends on the degree of coordination between galaxy age and galaxy formation rate. We find that early-type galaxies formed at least 11 Gyrs ago if their time of formation was 1 Gyr or if the ratio of the spread in formation time to the characteristic time scale at formation is 0.3, similar to what has been found by Bower, Lucey & Ellis (1992) for Coma galaxies. However our result, which assumes an intrinsic scatter $\sqrt{2}$ times smaller than the observed scatter, makes a smaller look-back time extrapolation since galaxies in Cl0939+4713 are 6 Gyrs younger than present day ones. That is, the redshift of (early type) galaxy formation is greater than 1.5 for the adopted cosmology.

Please note that, using space based data, it is possible to measure galaxy colors with small errors (because of the fainter sky background in space), allowing one to put a stronger constraint on the lower limit of the galaxy age, and consequently an upper limit on the value of H_0.

5.4.2. Spirals

The color distribution of spiral galaxies markedly differs (as expected) from those of the other coarse and detailed types, because there are no blue ($g - r < 1$ or $r - i < 0.5$) early-type galaxies (Table 3 and Figure 2b). The dispersion in the $g - r$ and $r - i$ colors for spirals (0.14 and 0.15 mag respectively) is larger than the photometric accuracy, making these galaxies heterogeneous in colors, as the Coma spirals.

A closer inspection of the spiral color distribution shows that the Cl0939+4713 spirals do not have unusual colors in general, since they have the K-corrected colors of present day field spirals. However we note that the spirals in Coma's core are red, since no blue spirals have been found there (Andreon 1996a), and the same applies to other nearby clusters (Oemler 1992). Therefore the Cl0939+4713 spirals have an unusual color for their distance from the cluster center. This is the well known excess of blue galaxies first noted in the core of distant clusters by Butcher & Oemler (1984).

5.5. $J - H$, $H - K$ and visual $- K$ infrared colors

No differences have been found in the infrared $J - H$ and $H - K$ color distributions among the K selected sub-samples of ellipticals, lenticulars and spirals (there is no line for such quantities in Table 3). However the three types only count 6, 14, and 14 galaxies respectively. No difference has even been found between the E+S0 and S color distributions. All these color distributions have a dispersion compatible with the photometric accuracy (~ 0.15 mag at $K \sim 17.5$).

Surprisingly, the same applies to the $visual - K$ color, but for the marginal detection of a difference between S0s and Ss and between Es+S0s and Ss, as already noted by Stanford, Eisenhardt & Dickinson (1995).

5.6. Morphological segregation

There is no statistical evidence of a radial, density or nearest galaxy segregation, but there is a clear indication of the presence of a preferred direction, along or orthogonal to which the types are more or less dispersed, as in Coma (Andreon 1996a) and Perseus (Andreon 1994), giving a statistical confirmation to the visual impression previously pointed out (there is no line for r, ρ_{10} and d_1 in Table 3 but there are for y and θ; see also Figure 1).

This is the third case, out of three studied by us, in which the primary source of the morphological segregation is not the radial or density segregation, but the presence of a privileged direction. In Coma, the privilegied direction is also present in the velocity field (Biviano et al. 1996).

For the Coma and Perseus clusters, the privileged direction is aligned with the direction of the filament in which they are embedded (Andreon 1996a,b) and also with the position angle of the outer isophotes of the cluster X-ray emission (note their close correspondence with the chain of bright galaxies in Perseus and with the NGC 4938 group in Coma on the isophote maps of Schwarz et al. (1992) and White, Briel & Henry (1993)). The privileged direction of the type distributions in Cl0939+4713 seems to coincide with the major axis of the outer isophotes of the X-ray emission, even though it is ill defined because of the irregularity of these isophotes.

6. Summary of the results

The results of the quantitative analysis of magnitude complete samples of galaxies in Cl0939+4713 and in Coma, classified by the same method, using images of very similar resolution, selecting the samples in very similar pass-bands and limiting them at the same absolute magnitude, can be summarized as follows.

1) We confirm the ordinariness of the morphology of distant early-type galaxies in Cl0939+4713, suggested by DOBG from a visual examination of the appearance of these galaxies. Galaxies of a given Hubble type are similar to those of Coma in their surface brightness, ellipticity and e_4 profiles, and in the relative frequencies of the outer envelope classifications.

2) The cluster Cl0939+4713 is rich in spirals, twice as much as in Coma, but half than previously estimated. The ratio between Es and S0s is larger in Cl0939+4713 than in Coma.

3) Barred lenticular galaxies are *apparently* missing in Cl0939+4713. But the coarse sampling of the point spread function of the *HST* images makes the detection of a bar very difficult, and therefore their absence at high redshift have to be interpreted with caution.

4) There are no statistical differences between the global luminosity functions of Cl0939+4713 and Coma, both limited to $M_J = -19.8$ or $M_J = -19.3$ mag, our present magnitude limits for the two Coma samples. The same applies to the luminosity function of the types, as already suggested by DOBG.

5) The mean surface brightnesses of Es and S0s differ by the same amount in Cl0939+4713 and in Coma (S0s are 0.2 mag arcsec^{-2} brighter than Es). Both Hubble classes are separately homogeneous in J mean surface brightness. Thanks to Pahre, Djorgovski & de Carvalho's (1996) finding, our result implies that the E and S0 classes in Cl0939+4713 have the same mean surface brightness as the respective classes in Coma. Lenticulars have a brighter mean surface brightness than spirals in the core of Cl0939+4713, as in Coma's core, but at variance with the spiral population outside Coma's core. Please note that our early-types are brighter than the "ordinary" class of Capaccioli et al. (1992) and therefore that the homogeneity only concerns bright galaxies.

6) The Es have the same $\sim U - B$ and $\sim B - V$ rest-frame colors as S0s, and both classes are homogeneous in these colors (once the color-magnitude relation is subtracted) in Cl0939+4713. This is also true in Coma. These galaxies are at least 11 Gyrs old.

7) The color-magnitude relation for early-type galaxies in Cl0939+4713 has the same slope as in Coma, extending to the visible-blue and near ultraviolet what Stanford, Eisenhardt & Dickinson (1995) found for the visual and near infrared colors.

9) The Ss in Cl0939+4713 have the $\sim U - B$ and $\sim B - V$ restframe colors of present days field Ss, but are bluer than the spirals in Coma's core, since the latter are redder than the ones in the field and also than the ones outside Coma's core.

10) The morphological types in Cl0939+4713 are segregated in the same way as in Coma and Perseus, i.e. without a clear evidence for a density or clustercentric segregation, but revealing the presence of a privileged direction that coincides with the position angle of the major axis of the outer X-ray isophotes in the three clusters.

7. Conclusions

7.1. Es and S0s

From all points of view, the early-type galaxies in Cl0939+4713 share the properties of their local counterpart galaxies, from which they are indistinguishable, at least within our photometric and statistical errors and for the considered, mainly photometric, galaxy properties. Please note that E+A galaxies in Cl0939+4713 morphologically are spirals and not ellipticals (Belloni et al. 1995 and Sect. 4).

The only difference known to date between the Cl0939+4713 early-type galaxies and the local respective counterparts is their rest-frame $J - K$ colors (Stanford, Eisenhardt & Dickinson 1995). However, Stanford, Eisenhardt & Dickinson (1995) use Bower's (1992 and private communication) colors of Coma

galaxies as a reference sample, which show a systematic difference with respect to Recillas-Cruz et al.'s (1990) $J - K$.

Since there are no blue early-type galaxies (at least in the studied samples), the ancestors of early-types will first become red, which takes ~ 1 Gyr (Charlot & Silk 1994), and then will take the early-type morphological appearance. This implies that morphological components characterizing spiral galaxies, such as spiral arms, HII regions and dust in large quantity, need more than 1 Gyr to be made undetectable by whatever mechanism is operating in clusters if S galaxies change morphological type.

7.2. Ss

Given their distance from the cluster center, the spirals in Cl0939+4713 have unusual properties. Their frequency with respect to the other morphological types is higher than in present day clusters, their colors are similar to those of field spirals, much more than to those of spirals in the center of Coma-like clusters, which are red. Their spatial distribution and mean surface brightness are not typical of red or infalling (blue) spirals in Coma, since the Cl0939+4713 spirals are not overbright for their magnitude and do not avoid the cluster center. This suggests that, in Cl0939+4713, the blue spirals are just spirals with a normal star formation rate, as suggested by the optical colors of blue galaxies in many other distant clusters (Rakos & Schombert 1995; Rakos, Maindl & Schombert 1996).

Why are blue spirals with a normal star formation rate present in the core of distant clusters, but absent in the core of nearby Coma-like clusters?

Many authors, starting with Butcher & Oemler (1984), suggest that some kind of evolution is responsible for the disappearance of this blue population, which becomes red or undetected. However, the fading and/or destruction of the distant blue population, to make them undetected in present day clusters, seems unreasonable (Rakos & Schombert 1995), since most galaxies have to disappear. Changing morphological type seems even more unreasonable, because of the homogeneity of the photometric properties of early-type galaxies which implies that they are at least 11 Gyrs old.

In present day clusters, the lack of blue galaxies in the cluster core, the color distribution of spiral galaxies and many of their properties can be explained if spirals falling in clusters have a starbust due to the ram pressure in the hot gas (Bothun & Dressler 1986) that consumes the galaxy's gas reservoir. During the burst, these galaxies become bluer and brighter in mean surface brightness, then, shortly after the burst, they become as red as ellipticals (Charlot & Silk 1994), thus explaining the presence of red spirals in cluster cores. Furthermore, the existence of galaxies exhibiting spectral signatures consistent with the presence of intermediate age stellar populations (Couch & Sharples 1987; Lavery & Henry 1988, Dressler & Gunn 1992), and the previously listed photometric evidence for the blue starburst spirals in Coma, support this scenario. In a simplified view, during the galaxy's motion through the intracluster hot gas, the galaxy's gas is removed by ram pressure (Gunn & Gott 1972) and therefore its star formation is truncated, thus accounting for the lack of blue galaxies in the cluster core.

This scenario can also account for the presence of many blue galaxies in the core of distant clusters if the conditions for galaxy gas stripping are not satisfied, for example if the

intergalactic gas density is lower than the threshold for this stripping.

X-ray observations show that the gas density distribution in Cl0939+4713 (Schindler & Wambsganss 1996) is quite different from that in Coma, and the conditions for triggering the starburst are perhaps not realized. In the distant cluster 3C295, which instead possesses a low fraction of blue galaxies (Butcher & Oemler 1984), the gas density is high (Henry et al. 1979). Furthermore, the existence of nearby clusters with a high fraction of blue galaxies (e.g. Abell 1367) and of distant clusters with a low fraction of blue spirals (e.g. Cl0016+16), even in the sample studied by Butcher & Oemler (1984) suggests that our present interpretation of the excess of blue galaxies in distant clusters is a possible alternative to the evolutive interpretation of the Butcher-Oemler effect.

In order to test this working hypothesis, we are now directly measuring the cluster gas brightness (which is a measure of the gas density) in a uniform way for a sample of clusters, nearby as well as distant, for which an accurate and uniform measure of the blue fraction of galaxies is available.

7.3. Morphological segregation

Sandage (1990) suggested testing whether the segregation is the result of a biased galaxy formation plus a current infall by measuring an evolution of the morphological segregation. In such a case, ellipticals form in high density regions whereas spirals in lower ones, which more recently detached from the Hubble flow and fall in the cluster. Therefore distant (younger) clusters have to be richer in ellipticals in their core than present day clusters, since their outer shells, richer in late type galaxies, have not yet fallen in.

However we have shown, in the detailed study of three cluster (Coma, Perseus and Cl0939+4713), that the galaxies are more strongly segregated with respect to a privileged direction than in density or clustercentric distance, making a simple verification of the above prediction more difficult. Furthermore, the core of Cl0939+4713 is poorer in early-type galaxies than Coma, showing that a more complex scenario is needed to explain the evolution of the galaxy populations in clusters.

A viable alternative for explaining why many distant clusters have higher spiral fractions than nearby ones is to remove the assumption that the former (or at least the observed ones) are the ancestors of the latter. This is reasonable, since it seems that distant and nearby clusters differ in richness and gas content. Therefore, the galaxy populations of distant clusters do not have to evolve necessarily into those of nearby ones. This resolves the problems encountered by evolutionary scenarios in accounting for the differences in galaxy populations observed in clusters at different redshifts.

References

Abraham R., Tanvir N., Santiago B. et al. 1996, MNRAS 279, L47

Andreon S., 1993, A&A 276, L17

Andreon S., 1994, A&A 284, 801

Andreon S. 1996a, A&A 314, 763

Andreon S. 1996b, PhD thesis, Université P. Sabatier, Toulouse, France

Andreon S., Davoust E. 1996, A&A, in press (astro-ph/9610235)

Andreon S., Davoust E., Poulain P., 1996a, A&AS, submitted

Andreon S., Davoust E., Michard R. et al. 1996b, A&AS, 116, 429

Aragón-Salamanca A., Ellis R., Couch W., Carter D. 1993, MNRAS 262, 764

Barrientos L.F., Shade D., Lópèz-Cruz O., 1996, ApJ 460, L89

Belloni P., Bruzual A., Thimm G., Röser H.-J., 1995, A&A 297, 61

Belloni P., Röser H.-J., 1996, A&AS, 118, 65

Biviano A., Durret F., Gerbal D., et al., 1996, A&A 311, 95

Bothun G., Dressler A., 1986, ApJ 301, 57

Bower R., Lucey J., Ellis R., 1992, MNRAS 254, 589

Butcher H., Oemler A., 1984, ApJ 285, 426

Butcher H., Oemler A., 1984, ApJS 57, 665

Capaccioli M., Caon N., D'Onofrio M., 1992, MNRAS 259, 323

Casertano S, Ratnatunga K., Griffits R. et al., 1995, ApJ 453, 599

Charlot S., Silk J., 1994, ApJ 432, 453

Coleman G., Wu C., Weedman D., 1980, ApJS 43, 393

Couch W., Sharples R. 1987, MNRAS 229, 423

Courteau S., de Jong R., Broeils A., 1996, ApJ, L73

Dressler A., 1980, ApJ 236, 351

Dressler A., Gunn J. 1992, ApJS 78, 1

Dressler A., Oemler A., Butcher H., Gunn J., 1994a, ApJ 430, 107

Dressler A., Oemler A., Sparks W., Lucas R., 1994b, ApJ 435, L23

Driver S., Windhorst R., Griffits R., 1995, ApJ 453, 48

Ellis R., 1996, in *Unsolved Problems in Astrophysics*, eds. J. Ostriker and J. Bahcall, Princeton, in press

Fukugita M., Shimasaku K., Ichikawa T., 1995, PASP 107, 945

Garilli B., Bottini D., Maccagni D., et al., 1996, ApJS 105, 191

Glazebrook K, Ellis R., Santiago B., Griffits R., 1995, MNRAS, 275, L19

Godwin J., Metcalfe N., Peach J., 1983, MNRAS 202, 113

Gunn J., Gott J., 1972, ApJ 176, 1

Henry J., Branduardi G., Fabricant D., et al., 1979, ApJ 234, L15

Holtzman J.,Burrows C., Casertano S. et al. 1995, PASP 107, 1065

Hubble E., 1936, *The Real of the Nebulae*, New Haven: Yale University Press

Kormendy J., 1977, ApJ 218, 333

Lavery R., Pierce M., McClure R., 1992, AJ 104, 6

Lavery R., Henry J., 1988, ApJ 330, 596

Michard R., Marchal J. 1993, A&AS 98, 29

Michard R., Marchal J. 1994, A&A 105, 481

Oemler A., 1992, in *Cluster and Supercluster of Galaxies*, eds. A. Fabian, (Kluwer Academic Publishers)

Pahre M., Djorgovski S., de Carvalho R., 1996, ApJL 456, 79

Poulain P., Nieto J.-L., Davoust E., 1992, A&AS 95, 129

Rakos K, Schombert J., 1995, ApJ 439, 47

Rakos K., Maindl T., Schombert J., ApJ, 1996, 466, 122

Recillas-Cruz E., Carrasco L., Serrano A. et al., 1990, A&A 229, 64

Saglia R., Bender R., Dressler A., 1993, A&A 279, 77

Sandage A., 1961, *The Hubble Atlas of Galaxies*, (Washinton: Carnegie Institution)

Sandage A., 1990, in *Clusters of Galaxies*, eds. W. Oegerle, M. Fitchett & L. Danly (Cambridge University Press)

Schindler S., Wambsganss J., 1996, A&A, 313, 113

Schwarz R., Edge A., Voges W., et al. 1992, A&A 256, L11

Seitz C., Kneib J.-P., Schneider P., Seitz S. 1996, A&A, 314, 707

Smail I., Hogg D., Yan L., Cohen J. 1995, ApJ 449, L105

Stanford S., Eisenhardt P., Dickinson M., 1995, ApJ 450, 512

Thompson L., 1986, ApJ 306, 384

van den Bergh S.,, Abraham R., Ellis R., et al. 1996, AJ, 112, 359

de Vaucouleurs G., 1959, *Handbuch der Physik*, vol. 53, (Berlin: Springer Verlag)

de Vaucouleurs G., Buta R., 1980, ApJS 44, 451

Visvanathan N., Sandage A., 1977, ApJ 216, 214

Zepf S., 1996, in *Sant'Agata Conference on Interacting Galaxies: in Pairs, Groups, and Clusters*, eds. G. Longo, M. Capaccioli, Busarello (Kluwer Academic Publishers)

White S., Briel U., Henry J., 1993, NMRAS 261, L8

Legend and notes of Table 1

Content of Table 1 (1) No in the Dressler & Gunn (1992) catalogue.

(2) logarithm of the approximate effective radius **in arcsec**.

(3) Photometric evidence for a disk, coded as: . st strong . cl clear . ft faint . no none.

(4) Typical axis ratio, either its minimum value, if clearly defined, or its value at the effective isophote in other cases.

(5) Location where the typical axis ratio was estimated, coded as ex for the extremum, re for the effective isophote, co if the value is the same at both locations.

(6) Typical e_4 parameter, either its extremum value, if clearly defined, or its value at the effective isophote in other cases. The estimates are in %.

(7) Location where the e_4 parameter was estimated, coded as ex for the extremum, re for the effective isophote, co if the value is the same at both locations.

(8) Axis ratio in the envelope, i.e. at the isophote $F702W \sim 25$ mag arcsec^{-2}.

(9) Amplitude of isophotal twist in the range of reliable measurements, in degrees. A dash means that the twist is difficult to be measured, as the isophotes are nearly circular.

(10) Detection of a bar, coded as follows: bar (bar seen), bar? (bar suspected), -no (no bar seen).

(11) Detection and classification of a disk, coded as follows: emDi (embedded disk), miDi (mixed disk), exDi (extended disk), -?Di (detected but unclassified disk), -no- (no disk seen).

(12) Detection of a spiral pattern, coded as follows: spiP (spiral pattern seen), spiP? (spiral pattern suspected), -no- (no spiral pattern seen).

(13) Classification of an envelope, coded as follows: spH (spheroidal halo), thD (thick disk), exD (extended disk), pec (peculiar envelope), -?- (unclassified envelope).

(14) Our morphological classification, coded as follows: boE (boxy E), unE (undetermined E), diE (disky E), SA0, SAB0, SB0, Sa, ... (as usual), S (spiral of unknown stage), SB.. (barred spiral of unknown stage).

(15) An asterisk refers to notes about specific features such as important dust pattern, ring or lens, low SuBr, f_4-asymmetry, etc. and about uncertainties of various sources.

NB: When parameters have not been measured or specific morphological components have not been studied, the relevant codes are replaced by blanks.

Notes to galaxies:

137 roundish galaxy, pear-shaped at intermediate radii, large twist in the envelope. SA0 galaxy with dust unresolved?

138 very irregular isophotes.

150 asymmetric in the outer regions.

190 irregular isophotes.

191 warp.

211 probably barred.

215 possible error of Dressler et al. (1994) in *HST* WF-PC1 identification.

225 irregular isophotes, HII regions.

269 uncertain type, because near the edge of the image.

292 more concentrated than DG 385.

293 arms and HII regions.

294 HII regions.

299 outer irregular isophotes.

302 difficult case, $r^{1/4}$ SuBr profile, boxy if anything.

310 various clumps superposed.

311 interacting, dust, ring.

312 arms and HII regions.

316 arms and HII regions.

318 within the halo of DG 311 - tidal extension.

320 arms, HII regions and dust.

329 HII regions, dust.

339 pear-shaped isophotes ($e3, f3 \neq 0$) at the r_e.

348 arms - beautiful spiral, HII regions.

360 edge-on, warped.

363 tail at low subr, difficult classification due to the smallness of the galaxy.

365 pear-shaped at low SuBr, nearby straight object (arclet?) and a galaxy at 1".

366 boxy bulge, f_4 asymmetry.

367 boxy inside 1 arcsec.

371 arm, HII regions.

375 strange companion galaxy(?).

377 larger component of pair probably unresolved from WF1.

383 arms.

384 S? irregular isophotes - dust?

385 $r^{1/4}$ profile, unresolved.

393 near the edge of the image.

397 superposed stars probably explain WF1 classification.

400 roundish galaxy.

408 slight evidence for a disk.

409 elongated galaxy with flat profile.

413 roundish galaxy with $r^{1/4}$ profile, irregular outer isophotes, and constant positive e_4.

422 non-concentric isophotes, tidal extension, possibly interacting with DG 439.

431 the companion galaxy DG 436 shows disturbances.

432 $r^{1/4}$ profile but asym. isophotes similar to the GMP 1646 irregular galaxy in Coma, difficult classification.

434 irregular asymmetric.

436 possibly interacting with DG 431, tidal extension, irregular isophotes, halo offcentered.

439 arms and dust.

441 edge-on, type uncertain because small asymmetry points toward S.

448 faint galaxy.

451 HII regions, possibly interacting with DG 458 because common envelope.

454 asymmetric.

457 face-on, two-component galaxy (bulge+disk).

458 roundish object, possibly interacting with DG 451.

462 irregular isophotes.

471 dust.

Table 1. Photometric parameters and classification of the galaxies in the sample

(1)	(2)	(3)	(4)	(5)	(6)	(7)	(8)	(9)	(10)	(11)	(12)	(13)	(14)	(15)
135											spiP	–	S	
137	-0.5	no	0.98	re	0.0	re	0.80	30	-no	-no-	-no	–	Pec	*
138												–	Irr	*
141													Sd	
150											spiP		S	*
190											spiP		S	*
191	-0.5	st	0.63	re	7.3	ex	0.44	7	-no	miDi	-no	thD	SA0	*
215	–	st	0.50	ex	-2.0	ex	0.60	7	-no	–	-no	spH	SA0	*
225													S	*
231													Irr	
246	-0.4	st	0.62	ex	3.0	ex	0.63	10	bar?	miDi	-no	thD	SAB0	
250	-0.7	cl	0.80	ex	0.0	re	0.85	5	-no	-?Di	-no	thD	SA0	
269	-0.4	no	0.90	co	0.0	co	0.96	–	-no	-no-	-no	–	unE	*
292													unresolved	*
293											spiP		S	*
294											spiP		Irr	*
299	-0.5	st	0.56	ex	4.9	ex	0.59	35	–		-no	-?-	SB..	*
302	–	cl	0.72	co	1.0	co	0.90	10	-no	emDi	-no	spH	SA0	*
303	-0.4	st	0.56	re	2.3	re	0.60	20	-no	miDi	-no	thD	SA0	
310	-0.3	cl	0.68	co	1.0	re	0.80	5	-no	emDi	-no	spH	SA0	*
311	0.3	cl	0.77	re	-2.6	ex	0.60	12	-no		-no	-?-	Pec	*
312													S	*
314	-0.6	ft	0.79	re	0.5	re	0.85	21	bar?	emDi	-no	thD	SAB0	
316													S	*
318	-0.3	cl	0.97	co	0.3	re	0.88	50	-no	exDi	-no	-?-	Pec	*
319	-0.6	ft	0.75	co	0.0	co	0.81	80	bar	–	-no	–	SB0	
320													S	*
321	-0.6	st	0.40	ex	6.6	ex	0.58	2	-no	-?Di	-no	spH	SA0	
322	-0.7	ft	0.71	ex	4.5	ex	0.79	12	-no	miDi	-no	thD	SA0	
329													S	*
336	–	st	0.48	–	2.0	–	0.71	15	–		-no	-?-	Irr	
338	-0.7	st	0.45	ex	5.9	ex	0.50	0	-no	miDi	-no	thD	SA0	
339	-0.2	no	0.80	re	-2.2	co	0.75	12	-no	-no-	-no	–	Pec	*
348													S	*
356	-0.8	st	0.58	ex	3.3	co	0.83	5	-no	emDi	-no	spH	SA0	
360	-0.3	cl	0.25	ex	10.3	ex	0.28	7				spH	S	*
361	-0.6	st	0.55	ex	2.6	ex	0.65	9	-no	miDi	-no	thD	SA0	
363	-0.7	st	0.62	ex	0.0	ex	0.75	0	-no	-no-	-no	thD	SA0	*
365	-0.6	st	0.43	ex	5.0	ex	0.46	7	-no	emDi	-no	spH	S	*
366	0.1	no	0.75	co	3.0	ex	0.77	5	-no	-?Di	-no	thD	diE	*
367	0.2	no	0.71	ex	-0.2	re	0.80	11	-no	-no-	-no	–	unE	*
371													S	*
375	–	st	0.39	ex	5.0	ex	0.51	3	-no	miDi	-no	thD	SA0	*
377	-0.5	st	0.38	ex	4.0	co	0.47	3	-no	emDi	-no	thD	SA0	*
381	-0.1	st	0.52	ex	1.9	ex	0.59	16	-no	emDi	-no	thD	SA0	
383											spiP		S	*
384	-0.5	st	0.54	ex	3.3	co	0.67	5	–		–	spH	unresolved	*
385													unresolved	*
389	-0.8	st	0.48	ex	7.0	co	0.57	3	-no	miDi	-no	spH	SA0	
393	-0.2	no	0.71	co	-1.0	re	-	0	-no	-no-	-no	–	boE	*
397	-0.5	cl	0.55	ex	3.4	ex	0.64	8:	-no	miDi	-no	thD	SA0	*
400	-0.6	no	0.93	co	0.0	co	0.91	20:	-no	-no-	-no	–	unE	*
408	-0.6	ft	0.74	co	2.8	co	0.69	10	-no	emDi	-no	thD	diE/SA0	*
409	–	st	0.21	–	0.5	–	0.45	3	–		-no	-?-	S	*
410	-0.6	st	0.39	ex	8.1	co	0.61	4	-no	miDi	-no	spH	SA0	
413	-0.4	no	0.85	co	1.7	re	0.85	0	-no	-no-	-no	–	diE	*
422	-0.3	st	0.82	re	-0.8	re	0.58	30	bar?		-no	–	S	*
425	-0.6	st	0.27	co	6.8	co	0.36	6	-no	emDi	-no	thD	SA0	
427	-0.2	no	0.68	co	-0.2	re	0.70	5	-no	-no-	-no	–	boE	
431	–	st	0.58	ex	3.6	ex	0.63	10	-no	emDi	-no	spH	SA0	*
432													Irr	*
434	-0.5	st	0.81	re	-3.1	ex	0.81	21	-no		-no	thD	Irr	*
436	-0.4	st	0.99	ex	0.0	re	0.91			–	-no	-?-	Pec	*
438	-0.5	st	0.48	ex	2.0	ex	0.64	10	-no	miDi	-no	spH	SA0	
439													S	*
441	-0.4	st	0.56	re	9.7	ex	0.31	5	-no	miDi	-no	thD	S	*

|													
443	-0.7	cl	0.69	ex	1.7	ex	0.83	10	-no	emDi	-no	spH	SA0
448	-0.8	no	0.95	co	0.0	co	0.95	–	-no	-no-	-no	–	unE *
451													Irr *
454											spiP		S *
457	-0.7	cl	0.91	ex	2.0	ex	0.92	–	-no	-?Di	-no	–	SA0 *
458	-0.3	no	0.98	co	0.0	co	0.96	–	-no	-no-	-no	–	unE *
462										bar?			S *
471											spiP		S *
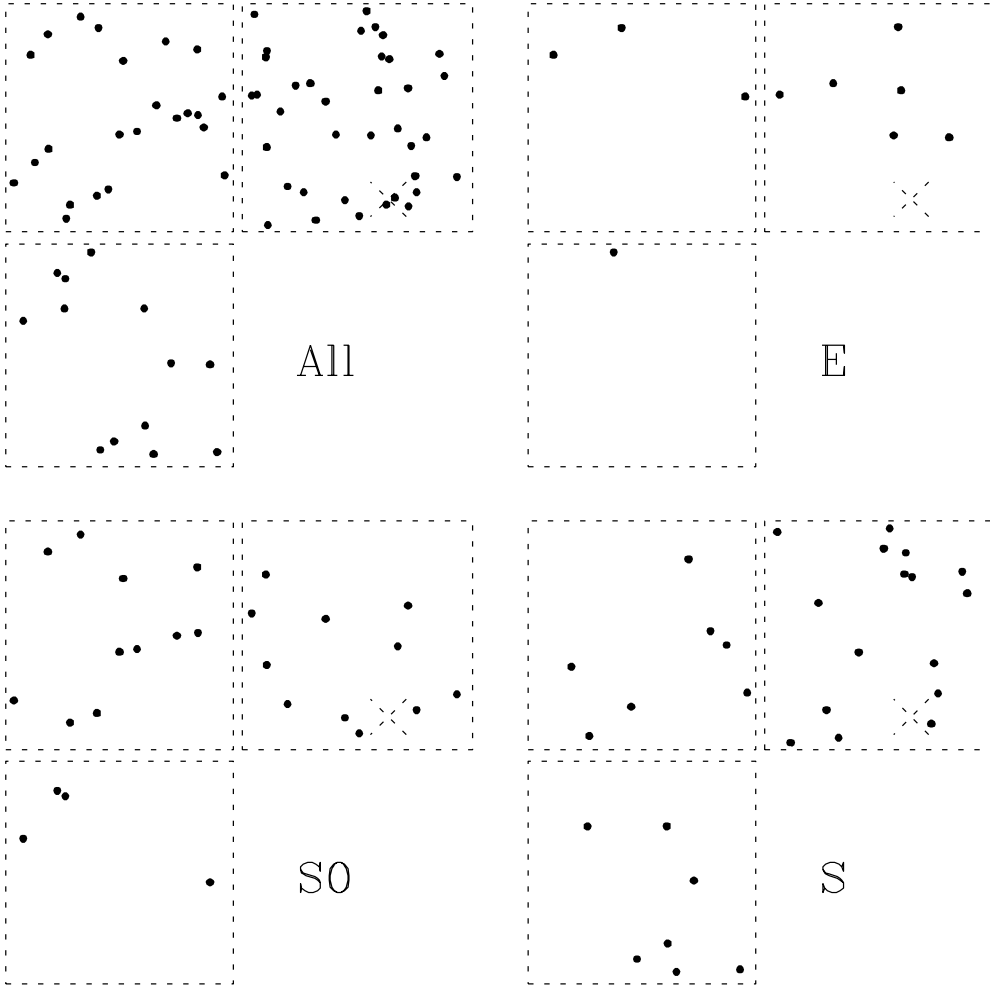
Fig. 1. Spatial distribution of all galaxies of Cl0939+4713 and of each individual Hubble type. North is up and East is left. Dashed lines delimitate the field of view of the three CCDs of the Wide Field Camera 2 of the *HST*. The cross marks the adopted cluster center. The x,y coordinate system used in this work is rotated 20 degrees clockwise with respect to the celestial coordinate system, to be aligned with the preferred direction outlined by the distribution of Es.
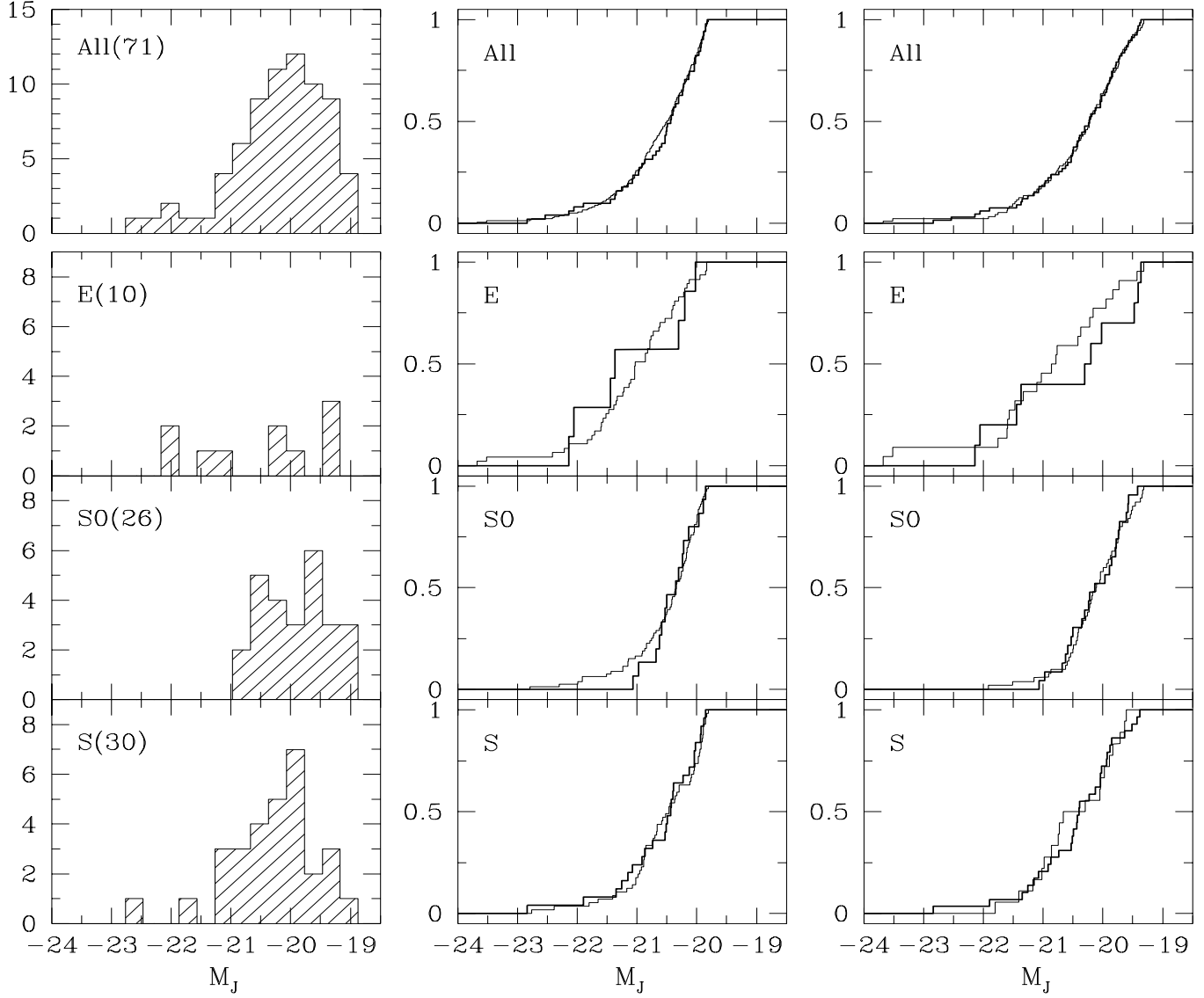
Fig. 2a. Left panel: J luminosity function of all galaxies of Cl0939+4713 and of each individual Hubble type. Central panel: comulative J luminosity distribution for galaxies brighter than $J = -19.8$ for Cl0939+4713 galaxies (thick line) and Coma-whole (thin line). Right panel: same as the central panel, but for a limiting magnitude $J = -19.3$ mag and for the comparison sample Coma-center.
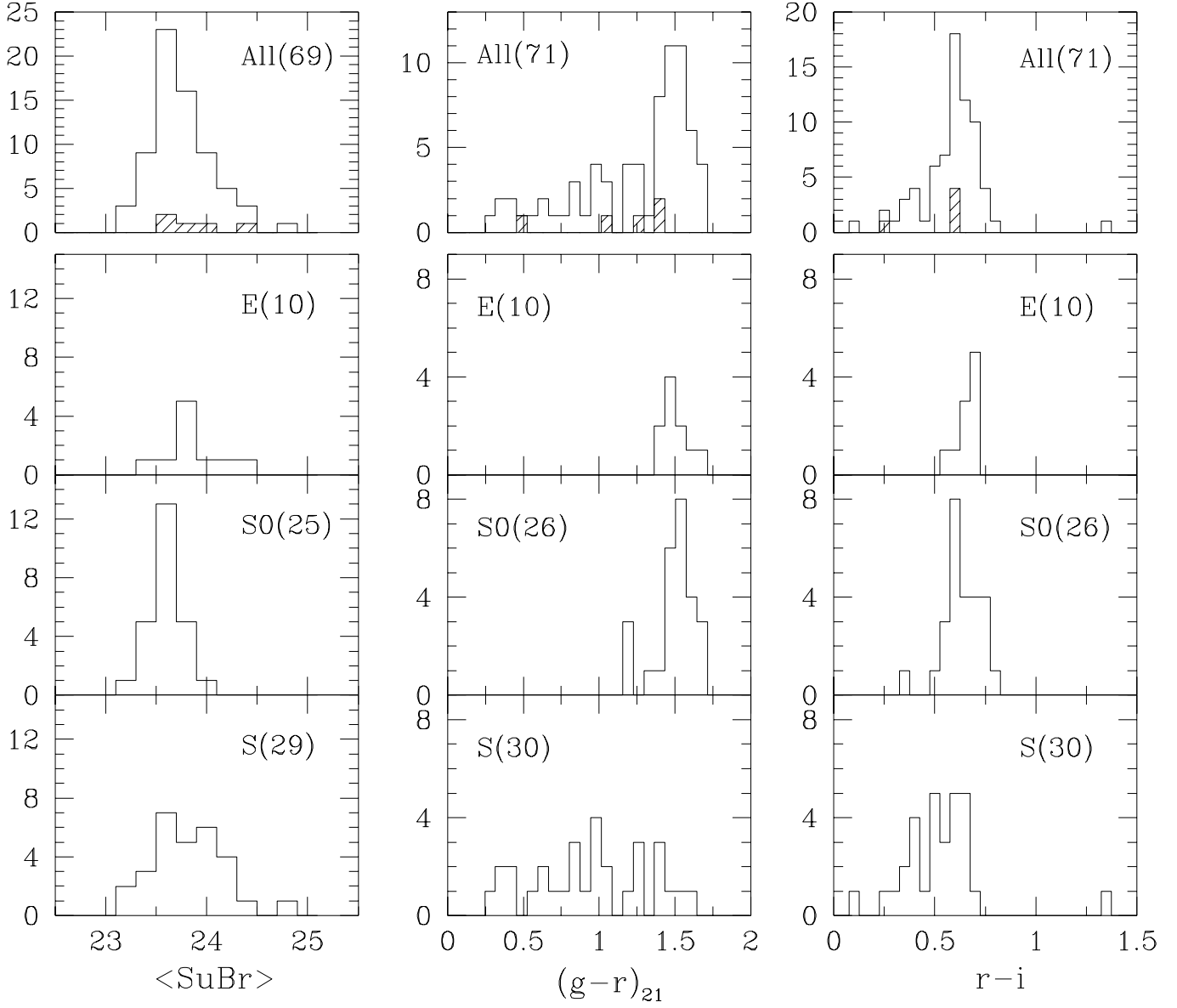
Fig. 2b. Mean apparent J surface brightness, $(g-r)_{21}$ and $r-i$ color distributions of all galaxies of Cl0939+4713 and of each individual Hubble type. The surface brightness is measured in mag arcsec^{-2}. $(g-r)_{21}$ is the $g-r$ color reduced to the magnitude $F702W = 21$ taking into account the color-magnitude relation. The hatched histogram in the top panels shows the distributions for peculiar or unresolved galaxies.